Published in final edited form as:
Int J Cancer. 2010 December 1; 127(11): 2598–2611. doi:10.1002/ijc.25281.

NK Depletion Results in Increased CCL22 Secretion and Treg Levels in Lewis Lung Carcinoma via the Accumulation of CCL22-secreting CD11b^{+}CD11c^{+} Cells

Mailloux, Adam W.,
Ralph H. Johnson VA Medical Center, Research Service; Medical University of South Carolina, Microbiology and Immunology

Clark, Anna-Maria A., and
Ralph H. Johnson VA Medical Center, Research Service; Medical University of South Carolina, Microbiology and Immunology

I. Young, M. Rita
Ralph H. Johnson VA Medical Center, Research Service; Medical University of South Carolina, Otolaryngology and Medicine

Abstract

Tumor induced immune suppression involves the accumulation of suppressive infiltrates in the tumor microenvironment such as regulatory T-cells (Tregs). Previous studies demonstrated that NK-dependant increases in CCL22 secretion selectively recruit Tregs toward murine lungs bearing Lewis Lung Carcinoma (LLC). In order to extend the in vitro studies, the present studies utilized *in vivo* depletion of NK cells to ascertain the contribution of NK-derived CCL22 toward total CCL22 and subsequent Treg levels in both normal and LLC-bearing lungs. However, NK depletion had the unexpected effect of increasing both CCL22 secretion and Treg levels in the lungs of NK-depleted LLC-bearing mice. This was concurrent with an increase in tumor burden. Flow cytometry and a series of both immunomagnetic and FACS isolations were used to identify the CCL22-producing cellular fractions in LLC-bearing lungs. A novel CD11b^{+}CD11c^{+} cell population was identified that accumulates in large numbers in NK-depleted LLC-bearing lung tissue. These CD11b^{+}CD11c^{+} cells secreted large amounts of CCL22 that may overcompensate for the loss of NK-derived CCL22 in the lungs of NK-depleted LLC-bearing mice. Taken together these data suggest that NK cells play both a positive and negative role in the regulation of CCL22 secretion and, in turn, the recruitment of Tregs toward LLC-bearing lungs.

Keywords

Natural Killer Cells; Regulatory T-cells; Chemokines; Cancer; Immune Suppression

Address correspondence and reprint requests to Dr. M. Rita I. Young, Research Service (151), 109 Bee Street, Ralph H. Johnson VA Medical Center, Charleston, SC 29401-5799 USA; Tel: (843) 789-6707; Fax: (843) 876-5384; rita.young@va.gov..

Category: Tumor Immunology

Novelty: CCL22 is an important chemokine regulating the trafficking of Tregs toward the tumor microenvironment. These studies reveal that NK-mediated regulation of CCL22 secretion is dynamic in nature in that NK cells can also inhibit CCL22 secretion by preventing the accumulation of CD11b^{+}CD11c^{+} cells in tumor-bearing lungs. This is despite the upregulated CCL22 secretion by NK cells in the tumor microenvironment.

Disclosures:
The authors have no financial conflicts of interest

Introduction

Tumor-induced immune suppression remains the largest obstacle toward effective immunotherapies against cancer [1, 2]. While solid tumors employ numerous mechanisms to evade immune responses, most involve the accumulation of suppressive infiltrates in the tumor microenvironment. One of the most potent and well studied of these suppressive infiltrates is the regulatory T-cell (Treg) [3]. High Treg numbers have been correlated with the expression of CCR4-associated chemokines within tumor tissue [4], and one of these chemokines, CCL22, has been shown to actively recruit Tregs toward human ovarian carcinoma and is indicative of a negative prognosis [5].

Lewis Lung Carcinoma (LLC) is a murine squamous cell carcinoma derived from lung epithelial cells. Upon tumor formation, LLC elicits potent immune suppression [6], largely related to immune suppressive cytokines [7], suppressive myeloid infiltrates [8-10], and Tregs [11]. Particular attention should be paid to Tregs as these cells preexist at basal concentration throughout the body [12] and thus, likely play a role in the induction of the suppressive microenvironment. Recent *in vitro* studies were carried out investigating the CCR4/chemokine axis in selective Treg recruitment toward LLC-bearing lung tissue. These studies investigated the CCR4-associated chemokines CCL22, and CCL17. While low levels of CCL17 were secreted from both normal and LLC-bearing lung tissue, CCL22 secretion was highly upregulated in LLC-bearing lung tissue. These elevated levels of CCL22 were found to selectively recruit Tregs toward LLC-bearing lungs [13]. Interestingly, CCL22 was not secreted by the LLC cells themselves. Isolation of cellular fractions and ex vivo depletion studies revealed that a large percentage of the increased CCL22 secretion from LLC-bearing lung tissue originates from NK cells, and that NK cells taken from the lungs of LLC-bearing mice secrete more CCL22 than those taken from normal controls[13]. Despite the strong evidence suggesting that NK-derived CCL22 plays a large role in selective Treg recruitment toward LLC, *in vivo* depletion studies have yet to be done to confirm this mechanism.

The current study investigates the role of NK cells on CCL22 secretion and subsequent Treg levels by *in vivo* depletion of NK cells during LLC tumor growth. Because increased CCL22 secretion from LLC-bearing lungs is NK-dependant, it was intuitive to hypothesize that CCL22 secretion would be positively regulated by NK cells within the tumor-bearing tissue. However, the present study reveals that NK-mediated regulation of CCL22 secretion is more dynamic in nature and that compensatory mechanisms exist for CCL22 secretion and Treg recruitment in the absence of NK cells.

Materials and Methods

Cell culture

A metastatic cell line of LLC (LN7) was used in all experiments. LLC and normal mouse lung epithelial cells (MLE-12) were kept in culture medium (RPMI-1640 media, Invitrogen) supplemented with 10% fetal bovine serum (FBS), 100 U/ml penicillin, 100 μg/ml streptomycin, 0.02 M Hepes buffer, and 5×10^{-5} M β-mercaptoethanol). Cells were passed as needed just prior to confluence. The LN7 variant of LLC cells are non-adherent in culture and, thus, do not require trypsinization prior to passage.

Generation of LLC-bearing lung tissues

Single cell suspensions of 1.0×10^{7} cells/ml washed in Hank's Buffered Saline Solution (HBSS, Invitrogen) were prepared from LLC cell cultures that were in log phase. Female C57BL/6 mice were injected i.v. into the tail vein with 0.2 ml of phosphate buffered saline or LLC cell suspension resulting in the delivery of 2.0×10^{6} LLC cells per animal. In previous studies, mice were euthanized approximately 16-18 days later when signs of

labored breathing first appeared in the LLC injected animals [13]. However, with NK-depleted animals, signs of labored breathing generally appeared around day 12. Hence, day 12 post tumor inoculation became the end point for all groups. Lung tissue was harvested and placed in HBSS prior to subsequent assays, or was frozen into blocks in Optimum Cutting Temperature (OCT; Sakura) compound using liquid N_2.

In vivo depletion of NK cells

Mice were injected with 0.2 mg of anti-asialo GM1 antibody (Wako Pure Chemicals Inc.) i.v. into the tail vein concurrently with a PBS or LLC injection. Control animals received injections of 0.2 mg normal rabbit serum. Multiple injections resulted in anaphylaxis; hence, singular injections of anti-asialo GM1 were used. The effectiveness of NK depletion was tracked using flow cytometric analysis of $NK1.1^+CD49b^+$ cell levels in dissociates from the lungs of both normal and LLC-bearing mice.

Generation of conditioned media

For the generation of conditioned media from cell cultures, the cells were washed with HBSS three times before reconstitution in serum-free culture media. Cultures were left at 37°C overnight (16 hours). The following morning, the media was collected and filtered. For the generation of conditioned media from intact tissue, whole intact lungs were rinsed in PBS and placed overnight (16 hours) at 37°C in 12 ml of serum-free culture media. The following morning, the media was collected and filtered.

Enzyme-linked immunosorbent assays (ELISA)

CCL22 was measured in various conditioned media using Quantikine Immunoassay kits (R&D Systems) according to the manufacturer's instructions.

Dissociation of solid lung tissues

Following harvest, entire sets of both normal and LLC-bearing lungs were placed in an enzyme digest (1 μg/ml collagenase IV, 0.6 μg/ml hyaluronidase, 0.1 μg/ml DNAse; Sigma) dissolved in HBSS for 90 minutes at room temperature. Each specimen was then homogenized in a Stomacher™ 80 homogenizer (Seward) set on medium for 120 seconds. The resulting homogenate was then rinsed with HBSS and filtered to remove debris, resulting in single cell suspensions.

Preparation of splenocytes and bone marrow

Whole spleens were harvested from normal C57BL/6 mice and homogenized via a Stomacher™80 homogenizer (Seward) set on medium for 60 seconds. Red blood cells were lysed using ACK lysis buffer. Bone marrow aspirate was obtained from the femurs of mice and passed through a 40μm cell strainer (BD Falcon). Red blood cells were lysed using ACK lysis buffer.

Lung weight analysis

Following harvest, each set of lungs was washed with PBS and gently shaken to remove excess PBS drops. Each lung was then weighed. The amount of time utilized for weight analysis was minimized to maintain cell viability in subsequent assays.

Flow cytometry

Non-specific staining was blocked with FBS and 1 μl/1.0×10^6 cells of CD16/32 (BD PharmMingen) before staining with 5 μl of the following antibodies: PE-NK1.1, PerCP-CD4, (BD PharmMingen); PE-CD25, FITC-FoxP3, and FITC-CD49a (DX5), FITC-F4/80,

PE-Ly-6G/Gr-1, FITC-CD31, APC-CD11b, and PE-CD11c (eBioscience). Intracellular staining for FoxP3 required overnight fixation with fixation/ permeabilization solution (eBioscience). Asialo GM1 staining was achieved using anti-asialo GM1 rabbit antiserum (Wako Pure Chemicals Inc.), followed by a secondary incubation with goat FITC-F(ab)^2 anti-rabbit IgG (Jackson Immunoresearch). The extent and frequency of labeled cells was visualized using flow cytometry (FacsCanto; BD Biosciences).

Hematoxylin, eosin, and erythrosine staining of frozen tissue

Lung tissue was frozen in OCT, cryosectioned into 10 μm sections, and placed onto glass slides. Sections were then fixed in 10% Neutral Buffered Formalin (Fischer Scientific) for 5 seconds, and rinsed five times with tap water. The sections were then stained with hematoxylin for approximately five minutes, and rinsed again in tap water five times. The sections were then decolorized by dipping each slide five times in 0.25% acid alcohol (1.25 ml con. HCl in 500 ml 70% ethanol). The slides were then rinsed in tap water six times and dipped in 0.17M lithium carbonate (Sigma) ten times. Each slide was then rinsed in distilled water five times followed by ten rinses in 95% ethanol (Harleco). The slides were then placed in a mixture of eosin and erythrosine [0.1% Eosin Y, 0.2% Erythrosine B, and 5% glacial acetic acid (Sigma) in 95% ethanol] for 30 seconds. The slides were then dehydrated by rinsing ten times in 95% ethanol followed by 10 rinses in 100% ethanol. Finally, slides were placed in xylene for 30 seconds twice. Once dry, slides were mounted with Aquamount (Harleco) and visualized using light microscopy.

Immunofluorescent staining of frozen tissue sections

Lung tissue was frozen in OCT, cryosectioned into 10 μm sections and placed onto glass slides. Tissue sections were fixed in ice cold methanol for 10 min., and non-specific staining was then blocked using 2% donkey serum in PBS for 1 hour at room temperature. After being rinsed in PBS, 1:100 dilutions in PBS of primary antibodies (CD11b, eBioscience; CD11c, BD Pharmingen) were added to the slides and allowed to incubate overnight at room temperature in a moist environment. The slides were then washed in PBS and donkey FITC-F(ab)^2 anti-rabbit and donkey Rhodamine-F(ab)^2 anti-rat secondary antibodies (Jackson labs) were added at a dilution of 1:100 each in PBS and allowed to incubate for 45 min. in room temperature in the dark. Following secondary incubations, slides were then rinsed in PBS, counterstained with Hoechst dye (Sigma), and then washed with distilled H_2O and mounted using Vectashield fluorescent mount media (Vector Laboratories Inc.). Fluorescent staining was visualized microscopically.

Immunomagnetic isolation

CD11b and CD11c fractions were isolated from lung tissue homogenates using isolation kits (Miltenyi Biotec) according to the manufacturer's instructions. CD3 and CD31 fractions were isolated from lung tissue homogenates by incubating with biotin-conjugated primary antibodies for 15 min. on ice (biotin-CD3, biotin-CD31 eBioscience), followed by a secondary incubation with streptavadin microbeads (Miltenyi Biotec) for 15 min on ice. The labeled cells were then positively collected using LS magnetic columns (Miltenyi Biotec).

Isolation using FACS

CD11b$^+$ subpopulations were first immunoflourescently labeled as described above for flow cytometry and then washed with PBS containing 1 μg/ml propidium iodide (Molecular Probes, Eugene, OR). Sorting was performed using a Dako MoFlo High-Speed Cell Sorter (Becton Dickinson).

Statistics

Data was reported using the mean as a measure of central tendency ± standard error of the mean. To compare one variable condition between groups, the two-tailed Student's *t* test was used. Significance was reported in the 95% confidence interval.

Results

Injection with anti-asialo GM1 effectively depletes NK cells during LLC growth

CCL22 selectively recruits Tregs to the local tumor microenvironment [5]. However, in the murine LLC model, CCL22 is not secreted by cancer cells or normal epithelial cells, but rather in part by resident NK cells in the tumor-bearing tissue as suggested by *ex vivo* studies [13]. In order to investigate the role that NK cells have in LLC-associated CCL22 secretion, the present studies utilized anti-asialo GM1 antibody to deplete NK cells *in vivo* and then measured CCL22 and Treg levels.

Prior studies have utilized multiple injections of anti-asialo GM1 to deplete NK cells in various experimental models [14]. However, we observed anaphylaxis in animals that received multiple anti-asialo GM1 injections as well as in animals that received multiple control rabbit serum injections. Therefore, only one injection in each mouse was used to avoid anaphylaxis and to ensure proper experimental conditions.

The use of anti-asialo GM1 as a means to deplete NK cells in the lungs of normal and LLC-bearing mice was validated by demonstrating that asialo GM1 expression in lung dissociates is restricted to NK cells. Both normal and LLC-bearing lung dissociates were stained with anti-asialo GM1 antibody followed by a FITC-fluorescent secondary antibody. Flow cytometric analysis revealed that in normal and LLC-bearing lung tissue, asialo GM1 is largely restricted to $NK1.1^+$ cells (Figure 1, *a*). Importantly, treatment with anti-asialo GM1 may also deplete NKT cells which can also express NK1.1, or CD49b. However, in normal or LLC-bearing lung tissues, no significant population of cells exist that expresses both NK and T-cell markers[13], suggesting that NKT cells do not play a significant role within this tumor model system.

LLC-bearing animals injected with anti-asialo-GM1 displayed signs of labored breathing as soon as day 11, and averaging 12 days after tumor injection. This was considered the endpoint for all test groups and lung tissue was then harvested. Flow cytometric analysis of fluorescently stained dissociates demonstrates that NK cell numbers remain depleted after day 12 post LLC and anti-asialo GM1 injection (Figure 1, *b*).

Depletion of NK cells results in increased LLC tumor burden

Upon resection of the various lung tissues, it became apparent that LLC tumor growth was greatly affected by NK depletion, while no visible effect occurred in normal lung tissues after NK cell depletion. LLC-bearing lung tissue typically forms numerous, but distinct, nodules concentrating around the outside periphery of the lung tissue, where the vascular bed is thickest. However, in NK-depleted animals, nodules were absent despite obviously heavy tumor burden (Figure 2, *a*). The NK-depleted LLC-bearing lung tissue was also firm to the touch and felt as though it were a solid mass.

The apparent increase in tumor burden in NK-depleted animals was confirmed by lung weight. Each excised set of lungs was weighed following a brief rinse in PBS. NK depletion had no effect on the weight of normal rabbit serum-injected control tissue. LLC-bearing lungs injected with rabbit serum were slightly heavier than normal and NK-depleted normal lungs (p=0.002). However, NK-depleted LLC-bearing lungs were by far the heaviest,

weighing over twice as much as rabbit serum-injected LLC-bearing lungs ($p<0.001$) (Figure 2, *b*).

Histological analysis also revealed large increases in tumor burden associated with NK cell depletion. Rabbit serum-injected control LLC-bearing lung tissue displayed signs of invasion and moderately heavy tumor burden, yet rudimentary boundaries could be seen with each respective nodule. As such, many non-epithelial structures remained intact such as blood vessels and bronchioles. In NK-depleted LLC-bearing lung tissues, no distinct nodules could be discerned. Instead, heavy tumor burden permeated every structure suggesting heavy invasiveness. PBS and rabbit serum-injected normal control lungs displayed normal histology. NK depletion had no visible effect on lung histology in PBS-injected animals (Figure 2, *c*).

NK depletion paradoxically raises CCL22 levels in LLC-bearing mice

Because NK cells were identified as a major CCL22 secreting component of LLC-bearing lung tissue [13], it was hypothesized that NK depletion would result in a reduction of CCL22 secretion from LLC-bearing lung tissue. Interestingly, media conditioned by NK-depleted LLC-bearing lung tissue contained CCL22 levels that were twice as high as the levels in media conditioned with control LLC-bearing lung tissue (2,208 ±286 ng/ml vs. 1,414 ±229 ng/ml, $p=0.049$) (Figure 3). Media conditioned with control LLC-bearing lung tissue still contained higher CCL22 levels than media conditioned with the lungs of normal PBS and rabbit serum injected control animals (1,414 ±229 ng/ml vs. 715 ±59 ng/ml, $p=0.01$), consistent with previously observed increases in CCL22 secretion by LLC-bearing lungs [13]. Additionally, NK depletion had no significant effect on CCL22 secretion from normal PBS-injected lung tissue.

NK-depletion results in highly elevated levels of Tregs in LLC-bearing lung tissues

The elevated CCL22 secretion seen from NK-depleted LLC-bearing lung tissue was unexpected. However, CCL22 was previously implicated in selective Treg recruitment toward LLC-bearing lung tissue [13] and CCR4 expression and CCR4-associated chemokine levels have been repeatedly correlated with high levels of Tregs [4, 5, 15-18]. Hence, the levels of Tregs in NK-depleted LLC-bearing lungs were measured. In order to measure Treg levels, NK-depleted and control rabbit serum-injected lung tissues from both LLC-bearing and PBS-injected control animals were dissociated and immunoflourescently stained for CD4, CD25, and FoxP3. Treg levels were quantified as a percentage of the total CD4 compartment (Figure 4, *a*). Treg levels in LLC-bearing lung tissues were significantly higher than in both NK-depleted and rabbit serum-injected normal PBS control tissues (13±1% vs. 5.4±0.6% and 4.9±0.3% respectively, $p<0.001$) (Figure 4, *b*). Treg levels in NK-depleted LLC-bearing lung tissues were significantly higher than in normal rabbit serum-inject LLC-bearing lung tissues (20±2% vs. 13±1%, $p=0.005$) (Figure 4, *b*). For both rabbit serum-injected and NK-depleted LLC-bearing lungs, total $CD4^+$ levels were similar or higher than that for normal rabbit serum-injected or NK-depleted normal PBS control lungs.

Increased CCL22 secretion remains in the myeloid fraction of NK-depleted LLC-bearing lungs

The paradoxical rise in CCL22 secretion from NK-depleted LLC-bearing lungs leads to the hypothesis that another cell population may compensate for CCL22 secretion in the absence of NK cells within the LLC microenvironment. In an attempt to narrow down possible CCL22-secreting cells, immunomagnetic isolations of $CD11b^+$, $CD11c^+$, $CD3^+$, and $CD31^+$ cells were performed on lung tissue dissociates from animals injected with PBS or LLC along with rabbit serum or anti-asialo GM1. Following the isolations, each fraction was plated at equal cell numbers and allowed to incubate overnight to generated conditioned

media. CCL22 was not secreted in any significant amounts from $CD31^+$ fractions isolated from the lungs of any of the groups of mice (Figure 5). $CD3^+$ cells isolated from PBS and rabbit serum-injected normal control lungs secreted moderate amounts of CCL22 (466±43ng/ml). Lower CCL22 secretion from isolated $CD3^+$ cells taken out of both rabbit serum-injected and NK-depleted LLC-bearing mouse lungs, as well as PBS-injected NK-depleted mouse lungs indicated that endogenous T-cells do not compensate for the loss of NK-derived CCL22 in NK-depleted LLC-bearing lung tissue. CCL22 secretion from isolated $CD11c^+$ fractions was moderately high from both rabbit serum-injected and NK-depleted PBS-injected control lungs (735±38ng/ml, and 776±21ng/ml respectively). CCL22 secretion from isolated $CD11c^+$ fractions was less moderate from both rabbit serum-injected and NK-depleted LLC-bearing lungs (429±66ng/ml and 465±136ng/ml, respectively).

Isolated $CD11b^+$ fractions displayed the most interesting results (Figure 5). $CD11b^+$ cells taken from both rabbit serum-injected and NK-depleted PBS-injected control lungs secreted very low amounts of CCL22 (155±51ng/ml and 94±30ng/ml, respectively). However, $CD11b^+$ cells taken from both rabbit serum-injected and NK-depleted LLC-bearing lungs secreted significantly higher levels of CCL22 (1,079±137ng/ml and 867±61ng/ml, respectively) than did $CD11b^+$ cells from either NK-depleted or rabbit serum-injected control lungs ($p<0.001$ across all four comparisons). Increased CCL22 secretion from $CD11b^+$ cells taken from LLC-bearing lungs issue is consistent with previous observations [13]. However, the fact that $CD11b^+$ cells taken from NK-depleted LLC-bearing lung tissue also display an increase in CCL22 secretion suggests that any cells compensating for lost NK-derived CCL22 still reside in the myeloid compartment. Because the isolated fractions were all plated at equal cell concentrations, this experiment does not take into account the relative frequencies of each fraction found in the various lung tissue types toward total CCL22 secretion.

$CD11b^+CD11c^+$ cells represent a novel component to the myeloid compartment in NK-depleted LLC-bearing lungs

In previous studies, two and three major $CD11b^+$ populations were identified in the $CD11b^+$ compartments of normal and LLC-bearing lungs respectively [13]. These populations were $CD11b^+NK1.1^+$ and $CD11b^+Gr\text{-}1^+$ cells in both normal and LLC-bearing lungs, along with the addition of $CD11b^+F4/80^+$ cells in LLC-bearing lungs. Within the myeloid fraction, these cellular markers were mutually exclusive from each other and accounted for the majority of the total $CD11b^+$ cells in both normal and LLC-bearing lungs [13]. However, these markers account for less than half of the total $CD11b^+$ fraction in NK-depleted LLC-bearing lungs suggesting that additional subpopulations are present.

A very large subpopulation was discovered within the myeloid compartment of NK-depleted LLC-bearing lung tissue that expresses both CD11b and CD11c (Figure 6). Amazingly, this population accounted for 45% of all $CD11b^+$ cells in NK-depleted LLC-bearing lung tissues. Additionally, this population is unique to NK-depleted LLC-bearing lung tissue as no $CD11b^+CD11c^+$ cells were detected in the lungs of either rabbit serum-injected or NK-depleted PBS-injected control animals. Minimal numbers were detected in rabbit serum-injected LLC-bearing lungs.

The uniqueness of $CD11b^+CD11c^+$ cells to NK-depleted LLC-bearing lung tissue was confirmed microscopically. Frozen lung sections from animals injected with PBS or LLC along with rabbit serum or anti-asialo GM1 were prepared and immunoflourescently stained for CD11b and CD11c. $CD11c^+$ cells were rare in lungs from PBS and rabbit serum-injected control animals, and were distinctly different from $CD11b^+$ cells (Figure 7, a). The same was true for $CD11c^+$ cells in the lungs of anti-asialo GM1 and PBS-injected animals (Figure 7, *b*), suggesting that cells that express both CD11b and CD11c are absent from these

tissues. Conversely, $CD11b^+CD11c^+$ cells could be found in rabbit serum-injected LLC-bearing lung tissue, although at miniscule frequencies (Figure 8, *a*). There was also a large increase in $CD11b^+$ cells that stained negatively for CD11c in the lungs of rabbit serum-injected LLC-bearing animals, reiterating previous observations of increased myeloid infiltration in LLC-bearing lung dissociates [13]. While $CD11b^+CD11c^+$ cells were rare in the lungs of rabbit serum-injected LLC-bearing animals, the lungs of anti-asialo GM1-injected LLC-bearing animals contained highly elevated levels of $CD11b^+CD11c^+$ cells (Figure 8, *b*). This suggests that high numbers of $CD11b^+CD11c^+$ cells may be unique to the lungs of anti-asialo GM1-injected LLC-bearing animals.

$CD11b^+CD11c^+$ cells secrete CCL22 in NK-depleted LLC-bearing lungs

We hypothesized that the paradoxical increase in CCL22 secretion seen in NK-depleted LLC-bearing lungs can be attributed to compensation by a novel cell population. Immunomagnetic isolations suggested that the majority of increased CCL22 secretion remained within the myeloid fraction in NK-depleted LLC-bearing lungs (Figure 5). However, a unique subpopulation of $CD11b^+$ cells that also express CD11c was identified in the lungs of NK-depleted LLC-bearing animals.

FACS was used to isolate each previously described $CD11b^+$ subpopulation along with this novel $CD11b^+CD11c^+$ fraction from lung dissociates from animals injected with PBS or LLC along with rabbit serum or anti-asialo GM1. Each isolated population of cells was plated at equal cell concentrations and allowed to incubate overnight to create conditioned media from which CCL22 secretion could be measured (Figure 9, *a*). Similar to previous observations [13], isolated $CD11b^+NK1.1^+$ cells from rabbit serum-injected LLC-bearing lungs secreted elevated levels of CCL22 compared to rabbit serum-injected PBS-injected control lungs (141±4 ng/ml vs. 53±4 ng/ml respectively, p=0.003). $C11b^+NK1.1^+$ cells were not present in anti-asialo GM1-injected PBS or LLC-bearing lungs. $CD11b^+Gr\text{-}1^+$ cells did not secrete detectable CCL22, nor did $CD11b^+F4/80^+$ cells isolated from rabbit serum-injected LLC-bearing lungs. Interestingly, no $CD11b^+F4/80^+$ cells were detected in anti-asialo GM1-injected LLC-bearing lungs, despite the fact that $F4/80^+$ cells do not stain positively for asialo GM1. No $CD11b^+F4/80^+$ cells were found in rabbit serum or anti-asialo GM1-injected PBS-injected control lungs.

Despite the low numbers of $CD11b^+CD11c^+$ cells found in rabbit serum-injected LLC-bearing lung tissue, enough cells were isolated to allow for CCL22 measurement. The $CD11b^+CD11c^+$ cells isolated from both rabbit serum and anti-asialo GM1-injected LLC-bearing lungs secreted moderate amounts of CCL22 (54±11 ng/ml and 67±8 ng/ml respectively). Each fraction was plated at equal cell concentrations in the experiment depicted in "part *a*" of Figure 9 and does not take the frequency of each population into account.

Prior to FACS isolation, a small aliquot was used to quantify the frequency of each subpopulation using flow cytometry. These frequencies were then used to adjust the measured amounts of CCL22 secretion in an attempt to better represent the CCL22 contribution of each fraction. The product of CCL22 and population frequency is depicted (Figure 9, *b*). Despite the fact that $NK1.1^+$ cells isolated from rabbit serum-injected LLC-bearing lungs secrete more CCL22 than $CD11b^+CD11c^+$ cells on a per cell basis, the relative contribution of $CD11b^+CD11c^+$ cells in NK-depleted LLC-bearing lung tissue is much greater due to highly elevated $CD11b^+CD11c^+$ cell numbers. Taken together, these data suggest that elevated $CD11b^+CD11c^+$ cell numbers in NK-depleted LLC-bearing lungs compensate for CCL22 secretion in the absence of NK cells.

$CD11b^+CD11c^+$ cells do not accumulate in bone marrow or secondary lymph tissue in LLC-bearing NK-depleted mice

While both CD11b and CD11c can be expressed on multiple cell types, the $CD11b^+CD11c^+$ cells accumulating in NK-depleted LLC-bearing lungs are likely myeloid dendritic cells (DC) distinct from lymphoid $CD11b^-CD11c^+$ DCs native to normal lung tissue. Unlike lymphoid DCs, myeloid DCs are of hematopoietic lineage originating from precursors in the bone marrow[19]. This raises the question if the observed $CD11b^+CD11c^+$ cell accumulation seen in NK-depleted LLC-bearing lungs is unique to tumor-bearing tissue within the tumor-bearing animals. In an effort to ascertain possible systemic accumulation, bone marrow and splenocytes were harvested from animals injected with PBS or LLC along with rabbit serum or anti-asialo GM1. The cells were then immunofluorescently stained for CD11b and CD11c and analyzed using flow cytometry. So significant changes were detected for $CD11b^+CD11c^+$ cell numbers across any group in either bone marrow (Figure 10, *a*) or spleen (Figure 10, *b*). This suggests that NK-depletion does not induce the accumulation of myeloid DCs in hematopoietic or secondary lymphoid tissues.

Discussion

Because NK cells secrete elevated levels of CCL22 and, consequently, recruit Tregs in the LLC microenvironment [13], we hypothesized that *in vivo* NK depletion would result in reduced levels of CCL22 secretion and Treg levels. Paradoxically, NK depletion resulted in a dramatic increase in CCL22 secretion from LLC-bearing lung tissue. This increase was not seen when NK cells were depleted from normal rabbit serum-injected controls suggesting that the phenomenon is unique to tumor-bearing individuals. While the increase in CCL22 secretion was unexpected, it became intuitive that increased levels of CCL22 would lead to increased numbers of Tregs. Indeed, NK-depleted LLC-bearing lung tissues contained highly elevated levels of Tregs that were approximately twice the levels in control rabbit serum-injected LLC-bearing lung tissue.

NK cells have a well established role in immune surveillance [20-23] and are generally accepted as a beneficial cell population for anti-tumor immunity. NK depletion at the time of tumor inoculation resulted in drastic increases in LLC tumor burden, suggesting that the positive anti-tumor role that NK cells play outweighs any detrimental role in supporting tumor-induced immune suppression. The increases in tumor burden seen here reiterate the importance of NK cells to the process of immune surveillance, and are not surprising despite the implications of NK-mediated Treg recruitment.

Given the paradoxical rise in CCL22 levels in NK-depleted animals, we hypothesized that NK depletion may alter the profile or behavior of infiltrating populations, resulting in one or more novel sources of CCL22 in LLC-bearing lungs. Here, we identified a large accumulation of $CD11b^+CD11c^+$ cells in NK-depleted LLC-bearing lungs that are absent in the lungs from both PBS-injected control groups and nearly absent from rabbit serum-injected LLC-bearing lungs. This novel population of cells secreted moderate amounts of CCL22 which, when taken in the context of the high numbers of $CD11b^+CD11c^+$ cells, largely overcompensates for the lost NK-derived CCL22. There is, however, a disjunction between the observed CCL22 secretion from FACS-isolated $CD11b^+CD11c^+$ cells and $CD11c^+$ cells isolated via immunomagnetic separation. $CD11c^+$ cells isolated from both rabbit serum and anti-asialo GM1-injected LLC-bearing lungs secreted less CCL22 than did $CD11c^+$ cells isolated from either rabbit serum or anti-asialo GM1-injected PBS control lungs. This is likely due to a lesser level of purity of isolated $CD11c^+$ cells from the immunomagnetic column. Of all the broad spectrum makers isolated via immunomagnetic separation, CD11c cells were the least enriched [13]. In addition, these cells would contain both $CD11c^+CD11b^+$ and $CD11c^+CD11b^-$ cells. Finally, following immunomagnetic

isolation, each cell fraction was plated at an equal concentration, meaning that the data collected in Figure 5 and "part *a*" of Figure 9 did not take cellular frequencies into account. Given the small prevalence of $CD11c^+$ cells in both rabbit serum and anti-asialo GM1-injected PBS control lungs, and in rabbit serum-injected LLC-bearing mice, it is not likely that $CD11c^+$-derived CCL22 is biologically significant. This is not true in NK-depleted LLC-bearing lung tissue, given the large cell numbers of $CD11b^+CD11c^+$ cell therein.

These results, combined with previous studies, suggest that NK-regulated CCL22 secretion is more complex than previously thought. Under normal circumstances, NK cells secrete minimal amounts of CCL22 in murine lungs. In the tumor microenvironment, this secretion is up-regulated by unknown factors, possibly IL-4 or IL-13, which can induce CCL22 secretion from NK cells *in vitro* [24]. At the same time, NK cells still play a positive role by inhibiting the accumulation of $CD11b^+CD11c^+$ cells which, at highly elevated cell numbers, contribute a larger pool of CCL22 than tumor-associated NK cells. Regardless, elevated levels of CCL22 lead to increased selective Treg recruitment and subsequent tumor-induced immune suppression (Figure 11).

The nature by which NK cells inhibit the accumulation of $CD11b^+CD11c^+$ is unknown. Given the ability of NK cells to produce both inflammatory cytokines and chemokines, it is easy to speculate that their absence alters both recruitment and induction mechanisms. It is also possible that NK cells may not directly inhibit the observed accumulation of $CD11b^+CD11c^+$ cells, but rather that anti-asialo GM1 may indirectly inhibit their accumulation by affecting other populations systemically, most notably NKT cells. However, detectable levels of NKT cells were not previously observed in either normal or LLC-bearing lungs[13].

A pressing question raised by these studies is the identity of the $CD11b^+CD11c^+$ cells accumulating in LLC-bearing lungs in the absence of NK cells. $CD11b^+CD11c^+$ cells have been described as an immature myeloid population in the normal continuum of myelopoietic differentiation [25]. The idea that the $CD11b^+CD11c^+$ cells found in NK-depleted LLC-bearing lungs are immature myeloid cells is consistent with observed detrimental effects of tumor influence on myelopoietic maturation [26], and would explain the lack of more mature myeloid populations such as $CD11b^+F4/80^+$ cells. Yet, if NK depletion adversely affects hematopoiesis, it is reasonable to expect $CD11b^+CD11c^+$ cell accumulation in the bone marrow as well. Since this is not the case, the most likely explanation is that this accumulation affects more mature myeloid populations. One common mature cell type that expresses both CD11b and CD11c is the myeloid DC[19]. These cells are distinct from lymphoid DCs in both origin and differentiation. As such they carry myeloid linage markers that are lacking in lymphoid DCs[19]. Interestingly, lymphoid DCs and myeloid DCs retain unique chemokine receptors and thus respond to entirely different recruitment signals based on distinct precursor cells[27]. By depleting NK cells, it is possible that the entire chemokine/cytokine milieu is shifted to one that favors the accumulation of myeloid DCs over resident lymphoid DCs. Further studies need to be conducted to verify the identity of these cells and their relationship to NK cells.

Acknowledgments

The authors would like to thank Dr. Amanda LaRue and HaiQun Zeng for their technical expertise and assistance with cell sorting. We are also grateful to Jennifer Konopa-Mulligan, and Jarrett Walsh for their support and assistance.

This work was supported by the Medical Research Service of the Veteran's Affairs and by the National Institute of Health grants R01CA8566, 1R01CA128837, and R01DE018168 (MRIY).

Abbreviations used in this article

Treg	Regulatory T-cell
LLC	Lewis Lung Carcinoma
MDSC	myeloid-derived suppressor cell
NK	Natural Killer Cell

References

1. Peterson AC, Harlin H, Gajewski TF. Immunization with Melan-A peptide-pulsed peripheral blood mononuclear cells plus recombinant human interleukin-12 induces clinical activity and T-cell responses in advanced melanoma. J Clin Oncol. 2003; 21:2342–8. [PubMed: 12805336]
2. Rosenberg SA, Sherry RM, Morton KE, Scharfman WJ, Yang JC, Topalian SL, Royal RE, Kammula U, Restifo NP, Hughes MS, Schwartzentruber D, Berman DM, et al. Tumor progression can occur despite the induction of very high levels of self/tumor antigen-specific CD8+ T cells in patients with melanoma. J Immunol. 2005; 175:6169–76. [PubMed: 16237114]
3. Sakaguchi S, Sakaguchi N, Asano M, Itoh M, Toda M. Immunologic self-tolerance maintained by activated T cells expressing IL-2 receptor alpha-chains (CD25). Breakdown of a single mechanism of self-tolerance causes various autoimmune diseases. J Immunol. 1995; 155:1151–64. [PubMed: 7636184]
4. Mizukami Y, Kono K, Kawaguchi Y, Akaike H, Kamimura K, Sugai H, Fujii H. CCL17 and CCL22 chemokines within tumor microenvironment are related to accumulation of Foxp3+ regulatory T cells in gastric cancer. Int J Cancer. 2008; 122:2286–93. [PubMed: 18224687]
5. Curiel TJ, Coukos G, Zou L, Alvarez X, Cheng P, Mottram P, Evdemon-Hogan M, Conejo-Garcia JR, Zhang L, Burow M, Zhu Y, Wei S, et al. Specific recruitment of regulatory T cells in ovarian carcinoma fosters immune privilege and predicts reduced survival. Nature medicine. 2004; 10:942–9.
6. Klykken PC, Munson AE. Immunosuppressive effects of the Lewis lung carcinoma. J Reticuloendothel Soc. 1979; 25:623–33. [PubMed: 385867]
7. Ippoliti F, Sezzi ML, Bellelli L, Naso G, Pontieri GM. Immunosubversive role of PGE2 in tumor bearing mice. Boll Ist Sieroter Milan. 1985; 64:25–34. [PubMed: 3859302]
8. Wiers K, Wright MA, Vellody K, Young MR. Failure of tumor-reactive lymph node cells to kill tumor in the presence of immune-suppressive CD34+ cells can be overcome with vitamin D3 treatment to diminish CD34+ cell levels. Clin Exp Metastasis. 1998; 16:275–82. [PubMed: 9568645]
9. Young MR, Newby M. Differential induction of suppressor macrophages by cloned Lewis lung carcinoma variants in mice. J Natl Cancer Inst. 1986; 77:1255–60. [PubMed: 3491925]
10. Young MR, Wheeler E, Newby M. Macrophage-mediated suppression of natural killer cell activity in mice bearing Lewis lung carcinoma. J Natl Cancer Inst. 1986; 76:745–50. [PubMed: 3457207]
11. Sharma S, Yang SC, Zhu L, Reckamp K, Gardner B, Baratelli F, Huang M, Batra RK, Dubinett SM. Tumor cyclooxygenase-2/prostaglandin E2-dependent promotion of FOXP3 expression and CD4+ CD25+ T regulatory cell activities in lung cancer. Cancer research. 2005; 65:5211–20. [PubMed: 15958566]
12. Baecher-Allan C, Viglietta V, Hafler DA. Human CD4+CD25+ regulatory T cells. Semin Immunol. 2004; 16:89–98. [PubMed: 15036232]
13. Mailloux AW, Young MR. NK-dependent increases in CCL22 secretion selectively recruits regulatory T cells to the tumor microenvironment. J Immunol. 2009; 182:2753–65. [PubMed: 19234170]
14. Suzuki K, Nakazato H, Matsui H, Hasumi M, Shibata Y, Ito K, Fukabori Y, Kurokawa K, Yamanaka H. NK cell-mediated anti-tumor immune response to human prostate cancer cell, PC-3: immunogene therapy using a highly secretable form of interleukin-15 gene transfer. Journal of leukocyte biology. 2001; 69:531–7. [PubMed: 11310838]

15. Haas J, Schopp L, Storch-Hagenlocher B, Fritzsching B, Jacobi C, Milkova L, Fritz B, Schwarz A, Suri-Payer E, Hensel M, Wildemann B. Specific recruitment of regulatory T cells into the CSF in lymphomatous and carcinomatous meningitis. Blood. 2008; 111:761–6. [PubMed: 17967942]

16. Iellem A, Mariani M, Lang R, Recalde H, Panina-Bordignon P, Sinigaglia F, D'Ambrosio D. Unique chemotactic response profile and specific expression of chemokine receptors CCR4 and CCR8 by CD4(+)CD25(+) regulatory T cells. The Journal of experimental medicine. 2001; 194:847–53. [PubMed: 11560999]

17. Ishida T, Ishii T, Inagaki A, Yano H, Komatsu H, Iida S, Inagaki H, Ueda R. Specific recruitment of CC chemokine receptor 4-positive regulatory T cells in Hodgkin lymphoma fosters immune privilege. Cancer research. 2006; 66:5716–22. [PubMed: 16740709]

18. Jordan JT, Sun W, Hussain SF, DeAngulo G, Prabhu SS, Heimberger AB. Preferential migration of regulatory T cells mediated by glioma-secreted chemokines can be blocked with chemotherapy. Cancer Immunol Immunother. 2008; 57:123–31. [PubMed: 17522861]

19. Vandenabeele S, Hochrein H, Mavaddat N, Winkel K, Shortman K. Human thymus contains 2 distinct dendritic cell populations. Blood. 2001; 97:1733–41. [PubMed: 11238115]

20. Dunn GP, Old LJ, Schreiber RD. The three Es of cancer immunoediting. Annual review of immunology. 2004; 22:329–60.

21. Girardi M, Oppenheim DE, Steele CR, Lewis JM, Glusac E, Filler R, Hobby P, Sutton B, Tigelaar RE, Hayday AC. Regulation of cutaneous malignancy by gammadelta T cells. Science (New York, N.Y. 2001; 294:605–9.

22. Smyth MJ, Crowe NY, Godfrey DI. NK cells and NKT cells collaborate in host protection from methylcholanthrene-induced fibrosarcoma. Int Immunol. 2001; 13:459–63. [PubMed: 11282985]

23. Smyth MJ, Thia KY, Street SE, Cretney E, Trapani JA, Taniguchi M, Kawano T, Pelikan SB, Crowe NY, Godfrey DI. Differential tumor surveillance by natural killer (NK) and NKT cells. The Journal of experimental medicine. 2000; 191:661–8. [PubMed: 10684858]

24. Andrew DP, Chang MS, McNinch J, Wathen ST, Rihanek M, Tseng J, Spellberg JP, Elias CG 3rd. STCP-1 (MDC) CC chemokine acts specifically on chronically activated Th2 lymphocytes and is produced by monocytes on stimulation with Th2 cytokines IL-4 and IL-13. J Immunol. 1998; 161:5027–38. [PubMed: 9794440]

25. Steptoe RJ, Ritchie JM, Jones LK, Harrison LC. Autoimmune diabetes is suppressed by transfer of proinsulin-encoding Gr-1+ myeloid progenitor cells that differentiate in vivo into resting dendritic cells. Diabetes. 2005; 54:434–42. [PubMed: 15677501]

26. Murdoch C, Muthana M, Coffelt SB, Lewis CE. The role of myeloid cells in the promotion of tumour angiogenesis. Nat Rev Cancer. 2008; 8:618–31. [PubMed: 18633355]

27. Osterholzer JJ, Chen GH, Olszewski MA, Curtis JL, Huffnagle GB, Toews GB. Accumulation of CD11b+ Lung Dendritic Cells in Response to Fungal Infection Results from the CCR2-Mediated Recruitment and Differentiation of Ly-6Chigh Monocytes. J Immunol. 2009; 183:8044–53. [PubMed: 19933856]

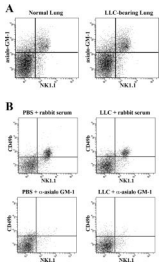

Figure 1.

NK cells remain depleted at 12 days after anti-asialo GM1 injection in both normal and LLC-bearing mice. (a) Asialo GM1 expression is restricted to $NK1.1^{+}$ cells in dissociates from both normal and LLC-bearing lung tissue. (b) Anti-asialo GM1 or normal rabbit serum control was injected into the tail veins of mice along with either LLC cells or PBS. After 12 days, NK cells remained effectively depleted in the lungs of anti-asialo GM1-injected animals.

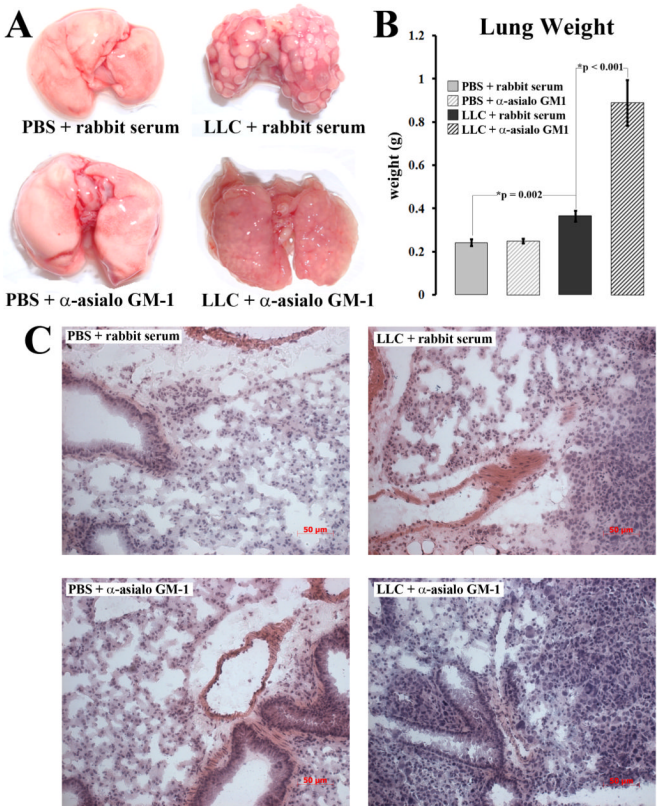

Figure 2.

NK depletion results in increased tumor burden. (a) Pictures of excised lungs from animals injected with LLC or PBS along with anti-asialo GM1 or normal rabbit serum. (b) Each excised group of lungs was weighed to approximate tumor burden. (c) Hematoxylin, Eosin, and erythrosine staining was performed on frozen cryosections from each group of lung tissues.

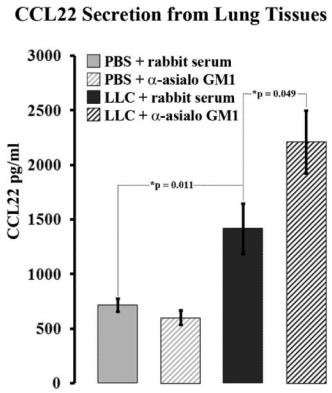

Figure 3.

NK depletion results in increase CCL22 secretion from LLC-bearing lung tissues. CCL22 levels were measured in media conditioned with resected lung tissue from animals injected with PBS or LLC along with rabbit serum or anti-asialo GM1.

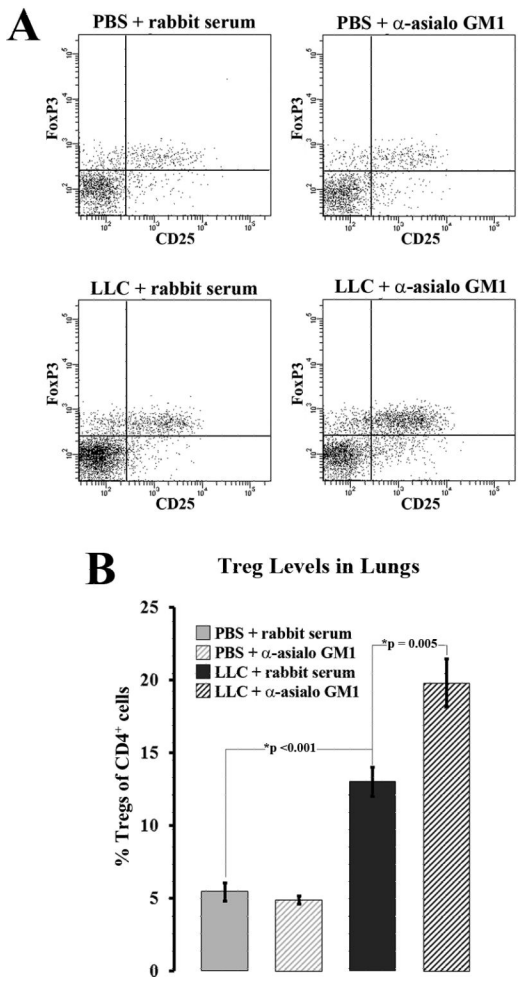

Figure 4.

Treg levels are increased in NK-depleted LLC-bearing lung tissues. (a) Dissociated lung tissue from animals injected with PBS or LLC along with rabbit serum or anti-asialo GM 1 was immunoflourescently stained for CD4, CD25, and FoxP3. Cells were first gated on CD4, and then $CD25^{+}FoxP3^{+}$ cells were quantified as Tregs. (b) Treg levels were measured as a percentage of the total $CD4^{+}$ compartment.

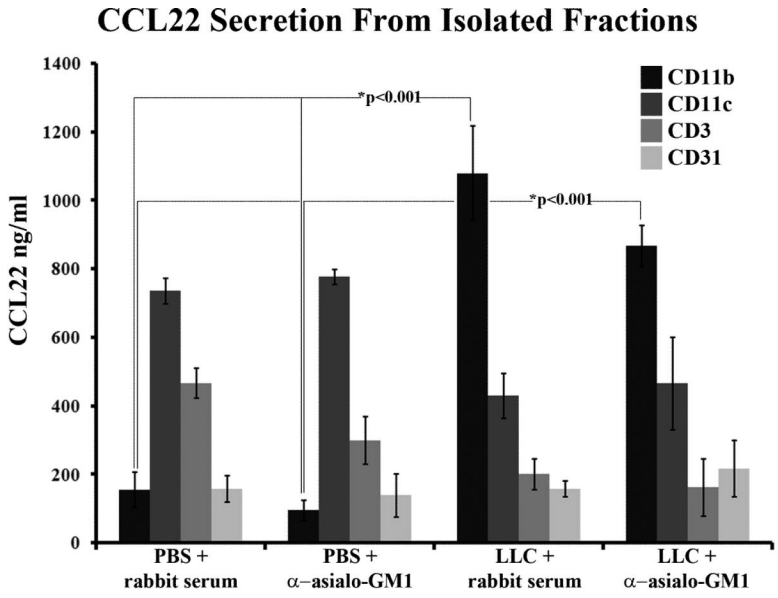

Figure 5.

Increased CCL22 secretion from NK-depleted LLC-bearing lung tissues appears restricted to the $CD11b^+$ fraction. $CD11b^+$, $CD11c^+$, $CD31^+$, and $CD3^+$ cells were immunomagnetically isolated and then incubated overnight at 1.0×10^6 cells/ml to create conditioned media. ELISA was then used on the various conditioned media to measure the levels of secreted CCL22.

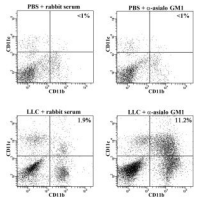

Figure 6.

$CD11b^{+}CD11c^{+}$ cells represent a novel component of the myeloid compartment in NK-depleted LLC-bearing lungs. Lung dissociates from animals injected with PBS or LLC along with rabbit serum or anti-asialo GM1 were immunoflourescently stained for CD11b and CD11c and analyzed using flow cytometry.

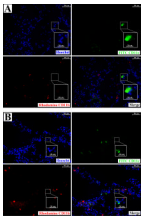

Figure 7.
CD11b and CD11c are expressed on different cells in normal lung tissues. Frozen sections from animals injected with PBS along with rabbit serum (a) or anti-asialo GM1 (b) were prepared and immunoflourescently stained with Hoechst dye (nuclear staining, top left), rhodamine-conjugated anti-CD11b (lower left), and FITC-conjugated anti-CD11c (top right). A merge of the three images is shown (lower right). Insets are of higher magnification of the indicated fields.

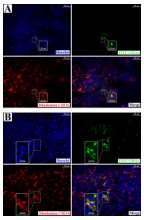

Figure 8.
$CD11b^{+}CD11c^{+}$ represent a unique population of cells in the lungs of NK-depleted LLC-bearing lung tissues. Frozen sections from LLC bearing animals injected with rabbit serum (a) or anti-asialo GM1 (b) were prepared and immunoflourescently stained with Hoechst dye (nuclear staining, top left), rhodamine-conjugated anti CD11b (lower left), and FITC-conjugated anti CD11c (top right). A merge of the three images is shown (lower right). Insets are of higher magnification of the indicated field.

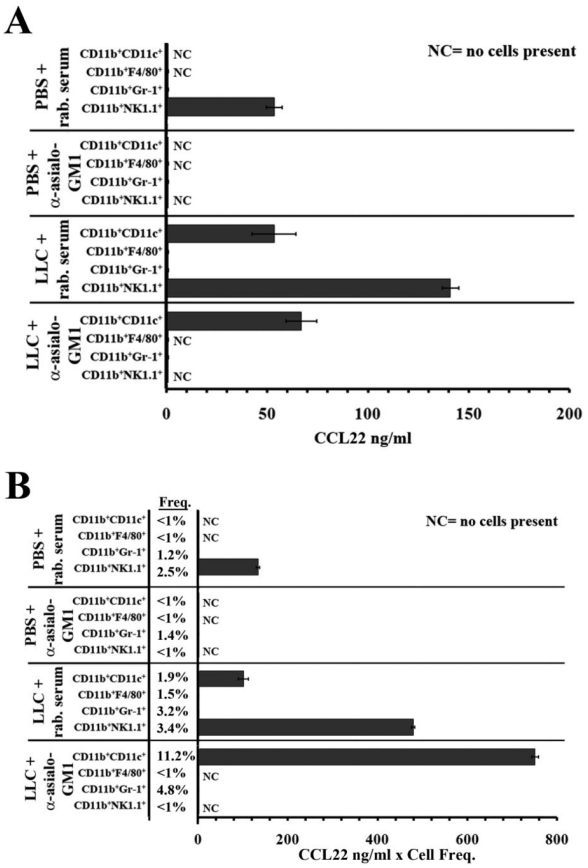

Figure 9.

$CD11b^+CD11c^+$ cells secrete CCL22 in NK-depleted LLC-bearing lung tissues. (a) Lung dissociates from animals injected with PBS or LLC along with rabbit serum or anti-asialo GM1 were immunoflourescently stained for CD11b, CD11c, Gr-1, F4/80, and NK1.1. Cells were first gated on $CD11b^+$ cells, and FACS was performed to isolate the $CD11b^+CD11c^+$, $CD11b^+NK1.1^+$, $CD11b^+Gr\text{-}1^+$, and $CD11b^+F4/80^+$ populations. The isolated fractions were then plated overnight at 5.0×10^5 cells/ml and ELISA was used to measure secreted CCL22 in the media. (b) CCL22 secretion of each fraction was multiplied by the population frequency (Freq.). Frequencies are reported as the percent of total lung dissociate.

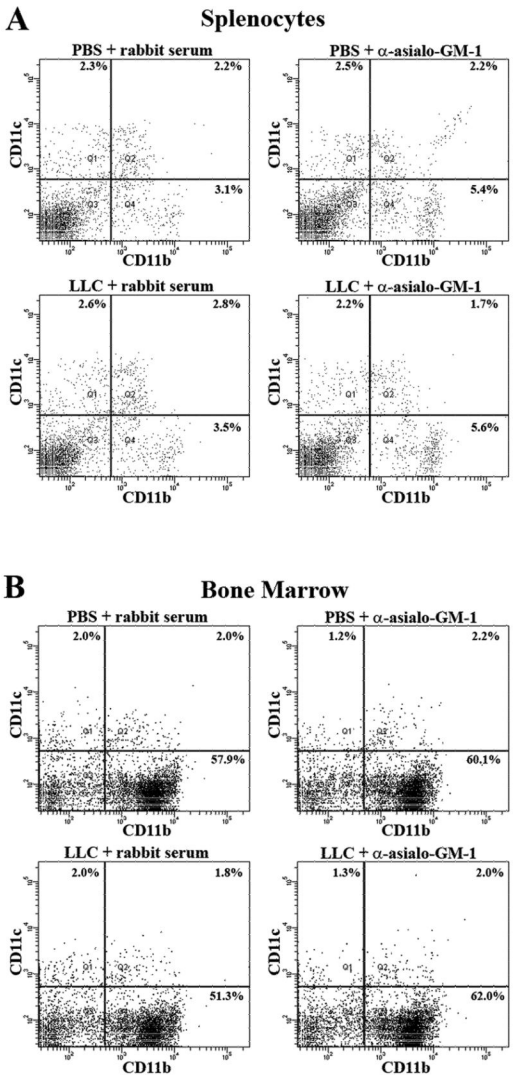

Figure 10.

Splenocytes (a) or bone marrow (b) that was harvested from animals injected with PBS or LLC along with rabbit serum or anti-asialo GM1 was immunofluorescently stained with CD11b and CD11c. The cells were then quantified using flow cytometry. No significant accumulation of $CD11b^{+}CD11c^{+}$ cells was seen in either spleen or bone marrow.

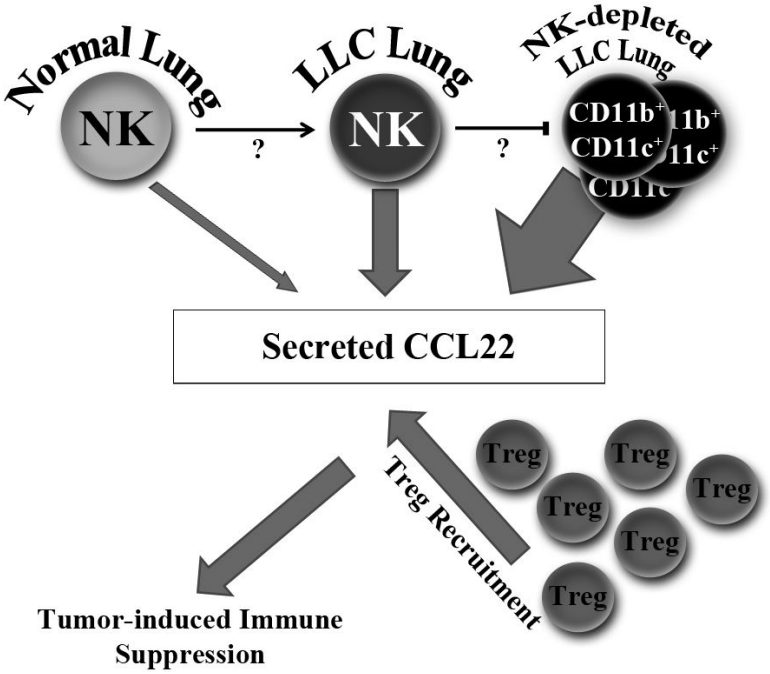

Figure 11.

NK cells play a dynamic role in the regulation of CCL22 secretion from murine lung tissue. Under normal circumstances, NK cells secrete minimal amounts of CCL22. However, NK cells in LLC-bearing lungs secrete elevated amounts of CCL22. Yet, NK cell presence in LLC-bearing lungs still plays a positive role by preventing even larger CCL22 secretion due to the emergence of $CD11b^{+}CD11c^{+}$ cells. Regardless of the source, increased CCL22 leads to increased Treg recruitment and subsequent tumor-induced immune suppression.